

MICROSTRUCTURE AND HARDNESS OF EXTRUSION WELDING ON HOLLOW PANEL AA6061 ALUMINUM ALLOY

Received – Priljeno: 2024-06-30
Accepted – Prihvaćeno: 2024-08-20
Original Scientific Paper – Izvorni znanstveni rad

Given the length of the structure, extruded products are occasionally joined to reach the desired length. To minimize production costs, this joint is achieved through extrusion welding, where it takes place while the workpiece is still a heated billet inside a chamber. As extrusion structures differ in complexity, this study seeks to identify the traits of extrusion welding outcomes across various structural designs. Research findings suggest that structural design significantly impacts both the physical and mechanical properties of the extruded plate and the extrusion joints.

Keywords: extruded aluminum, extrusion welding, complexity, microstructure, hardness

INTRODUCTION

Aluminum alloys have several beneficial characteristics, including being lightweight, highly resistant to corrosion, and having good thermal conductivity [1]. These properties make aluminum suitable for use in the transportation industry, particularly for manufacturing train car bodies [2,3]. Modern train car bodies are often produced through extrusion to create hollow panels [4]. This design choice helps reduce the car body's mass, enhancing speed and fuel efficiency. Given the length of trains, it is necessary to join hollow panels to form a continuous structure. Fusion welding is commonly used for this purpose [5].

Fusion welding involves using a heat source to melt the materials being joined, either with or without filler metal [6]. Its advantages include providing mechanical strength to the welded joint. However, uneven heat input can cause distortion and residual stress in the workpiece [7,8]. To reduce welding defects and minimize costs, improved welding methods for extruded hollow panels are needed. One such method is extrusion welding, which joins profiles during the extrusion process by heating a billet inside a container to 400-450°C [1,7]. This process can produce continuous profiles of the desired length [9].

The extrusion welding with longitudinal joints using aluminum alloy 2195 found that increasing the temperature and extrusion speed enhanced the closure of microvoids on the workpiece surface [10]. The quality of longitudinal extrusion joints is affected by the billet heating temperature, whereas higher temperatures improved welding joints. Due to the hollow panels are manufactured in many designs, this study focuses on the extrusion welding of aluminum 6061 hollow panel jo-

ints, examining profiles with varying levels of complexity. The aim is to investigate how different profile designs affect the physical and mechanical properties of the welded panels resulting from the extrusion process.

EXPERIMENTAL PROCEDURES

This study utilized extruded aluminum alloy 6061 hollow panels. The extrusion welding process involved joining two billets to create a continuous extrusion, as illustrated in Figure 1. Following the extrusion process, the profile shapes were categorized into three levels of complexity: simple, medium, and complex, as shown in Figure 2. These hollow panels were then prepared as plates and grouped based on the configuration of their sides: horizontal, vertical, and fin, as depicted in Figure 3.

After preparation, the specimens from the extrusion welding process were tested to determine their physical and mechanical properties. The tests included metallographic and hardness testing. Metallographic testing ai-

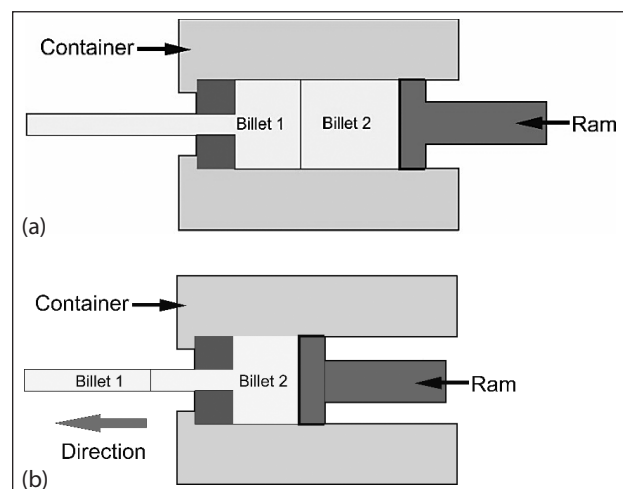


Figure 1 Extrusion welding illustration: (a) initial process, (b) joined panel

Triyono (e-mail: triyono74@staff.uns.ac.id), A. B. P. Sutowijoyo, E. D. W. S. Putri, N. Muhayat, A. R. Prabowo, Triyono, Mechanical Engineering Department, Universitas Sebelas Maret, Surakarta, Indonesia, Y. P. D. S. Dipari, National Research and Innovation Agency of Republic Indonesia (BRIN), Jakarta Pusat, 10340, Indonesia

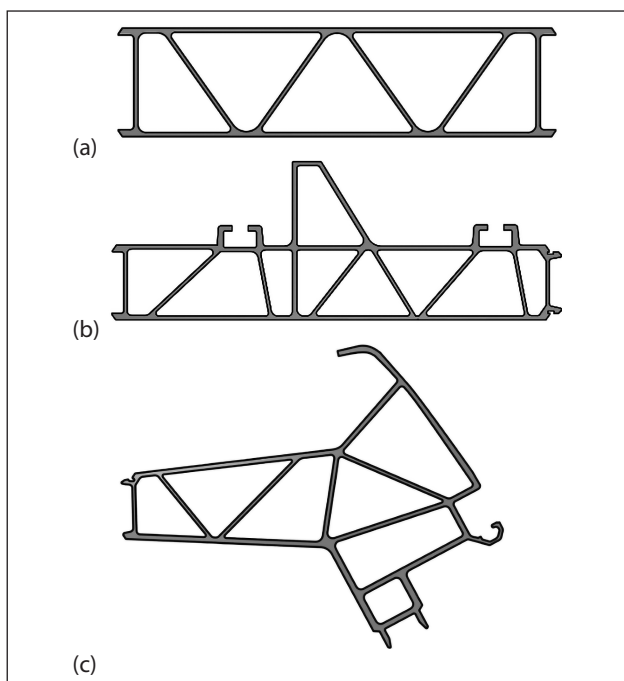


Figure 2 Detail geometry of extruded hollow panel profiles (a) simple, (b) medium, and (c) complex

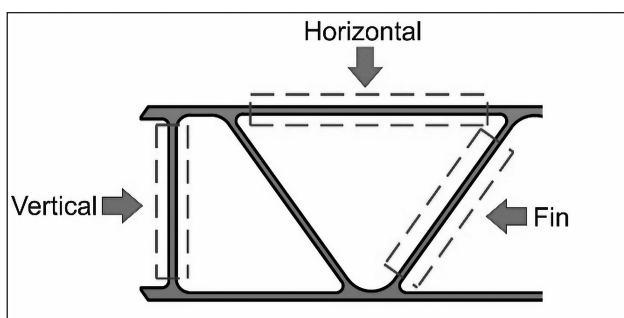


Figure 3 Terminology of the hollow panel sides

med to observe the macro and microstructures of the extrusion welding outcomes. For macrostructure observation, an Olympus SZ61 microscope was used, while an Olympus SZ2 ILST microscope was employed for microstructure observation. The specimens were etched using Keller reagent, which consists of 12 mL HF, 15 mL HCl, 25 mL HNO₃, and 90 mL distilled water, with an immersion time of 3 minutes. Following the macro and microstructure observations, the specimens underwent hardness testing using a Vickers microhardness machine, model HWMMT-X7, with 11 indentation points.

RESULTS AND DISCUSSION

Based on the micro and macrostructure observations of simple, medium, and complex hollow panels (Figures 5-7), distinct color patterns are evident in the macrostructure of each panel. These patterns, which differ between the outer and inner regions, arise from the cooling process after extrusion using a cooling etchant. The outer layer cools significantly faster than the inner layer, leading to temperature variations and resulting color differences, as shown in the macrostructure observations in Figures 4,5,6.

Microstructure observations reveal the absence of precipitates within the hollow panels. This absence indicates

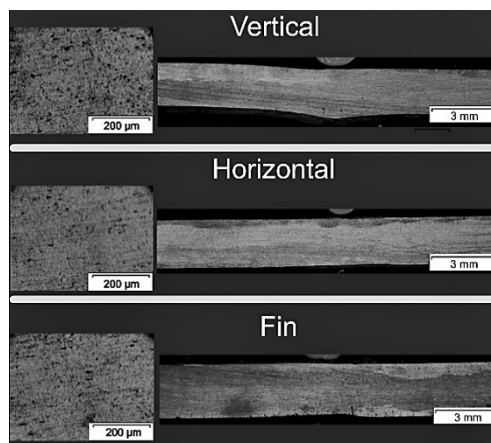


Figure 4 Microstructure of simple hollow panel

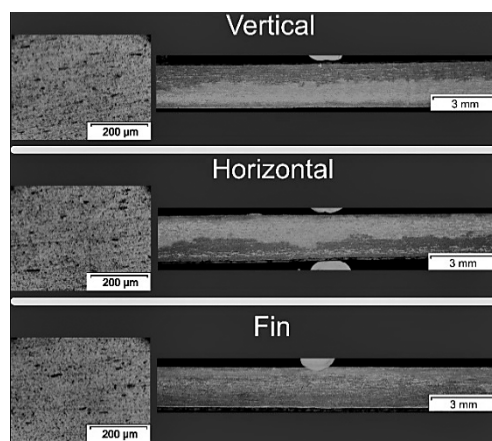


Figure 5 Microstructure of medium complexity of hollow panel

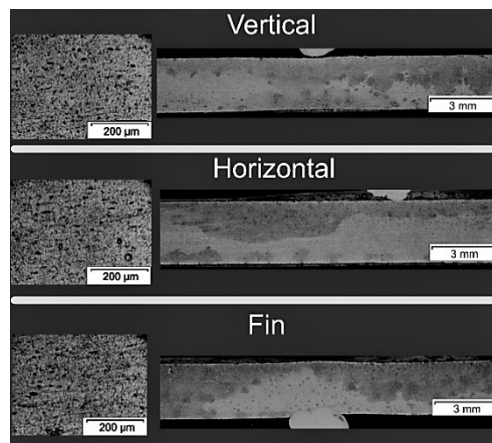


Figure 6 Microstructure of complex hollow panel

that phases which would normally precipitate during the initial heating phase of extrusion have dissolved [12]. The microstructures of simple and medium hollow panels exhibit similar grain shapes on each side, in contrast to the coarser grain structure found in the complex hollow panel. This difference is attributed to the increased pressure on the ram and friction between the billet and dies in more complex panels, affecting the temperature during extrusion and resulting in a coarser grain structure [13].

Hardness testing across each side of the hollow panels shows a relatively uniform distribution of values in both the Weld Zone (WZ) and Base Metal (BM) areas. For the simple hollow panel (Figure 7), the highest average hardness is on the fin side at 91.4 HV, while the lowest is on

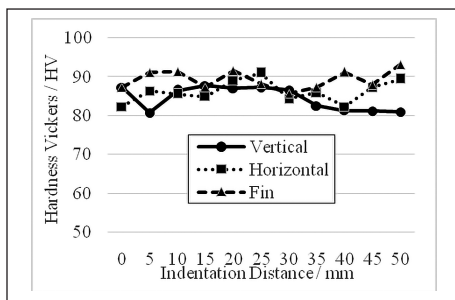


Figure 7 Hardness of simple hollow panel.

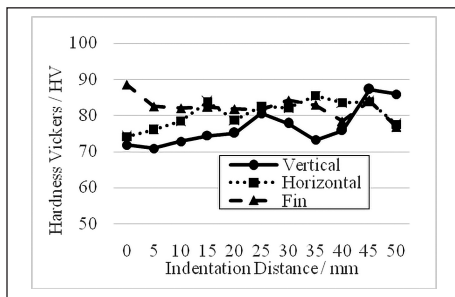


Figure 8 Hardness of medium hollow panel

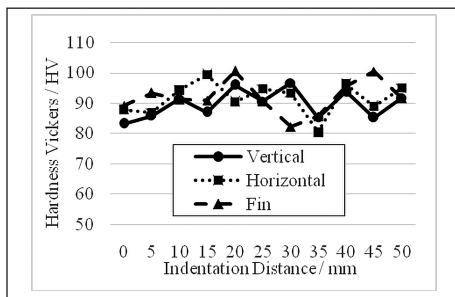


Figure 9 Hardness of complex hollow panel

the vertical side at 84.2 HV. The medium hollow panel (Figure 8) has its highest average hardness on the fin side at 81.58 HV and the lowest on the vertical side at 76.68 HV. The complex hollow panel (Figure 9) exhibits the highest average hardness value at 91.13 HV. This elevated hardness in the complex panel correlates with its coarser grain structure, as coarse grains typically have higher hardness values compared to finer grains [14].

CONCLUSIONS

Based on the results, the following conclusions can be drawn:

1. The complexity of the hollow panel influences the grain structure size. More complex hollow panels tend to have a finer grain structure.
2. A finer grain structure increases the hardness of the hollow panel. This is because the complexity of the panel increases the pressure on the ram and the frictional force on the die, leading to increase the level of strain hardening in billet.

ACKNOWLEDGMENTS

The authors are grateful to Badan Riset dan Inovasi Nasional (BRIN) Indonesia for financing this research through RIIM Grant, with contract no. 1562.1/UN27.22/

HK.07.00/2022 and all students in the METALS research group for assisting this research.

REFERENCES

- [1] K. V. Shivananda Murthy, D. P. Girish, R. Keshavamurthy, T. Varol, and P. G. Koppad, Mechanical and thermal properties of AA7075/TiO₂/Fly ash hybrid composites obtained by hot forging, *Prog. Nat. Sci.*, 27 (2017) 4, 474–481, doi: 10.1016/j.pnsc.2017.08.005.
- [2] Z. Liu, Y. Geng, M. Adams, L. Dong, L. Sun, J. Zhao, H. Dong, J. Wu, X. Tian, Uncovering driving forces on greenhouse gas emissions in China's aluminum industry from the perspective of life cycle analysis, *Appl. Energy*, 166 (2016), 253–263, doi:10.1016/j.apenergy.2015.11.075.
- [3] J. S. Kim and J. C. Jeong, Natural frequency evaluation of a composite train carbody with length of 23 m, *Compos. Sci. Technol.*, 66 (2006), 13, 2272–2283, doi: 10.1016/j.compscitech.2005.11.036.
- [4] J. Zhang, D. Yao, M. Shen, R. Wang, J. Li, and S. Guo, Effect of multi-layered IIR/EP on noise reduction of aluminium extrusions for high-speed trains, *Compos. Struct.*, 262, (2021), doi: 10.1016/j.comps truct.2021.113638.
- [5] A. Shrivastava, M. Krones, and F. E. Pfefferkorn, Comparison of energy consumption and environmental impact of friction stir welding and gas metal arc welding for aluminium, *CIRP J. Manuf. Sci. Technol.*, 9 (2015), 159–168, doi: 10.1016/j.cirpj.2014.10.001.
- [6] A. Abdollahi, M. Nganbe, and A. S. Kabir, On the elimination of solidification cracks in fusion welding of Al7075 by TiC-nanoparticle enhanced filler metal, *J. Manuf. Process.*, 81 (2022), 828–836, doi: 10.1016/j.jmapro.2022.07.039.
- [7] K. Vasu, H. Chelladurai, A. Ramaswamy, S. Malarvizhi, and V. Balasubramanian, Effect of fusion welding processes on tensile properties of armor grade, high thickness, non-heat treatable aluminium alloy joints, *Def. Technology*, 15 (2019) 3, 353–362, doi:10.1016/j.dt.2018.11.004.
- [8] H. Long, D. Gery, A. Carlier, and P. G. Maropoulos, Prediction of welding distortion in butt joint of thin plates, *Mater. Des.*, 30 (2009) 10, 4126–4135, doi: 10.1016/j.matdes.2009.05.004.
- [9] Q. Li, C. Harris, and M. R. Jolly, Finite element modelling simulation of transverse welding phenomenon in aluminium extrusion process, *Mater. Des.*, 24 (2003) 7, 493–496, doi: 10.1016/S0261-3069(03)00123-7
- [10] X. Xu, G. Zhao, S. Yu, Y. Wang, X. Chen, and W. Zhang, Effects of extrusion parameters and post-heat treatments on microstructures and mechanical properties of extrusion weld seams in 2195 Al-Li alloy profiles, *J. Mater. Res.*, 9 (2020) 3, 2662–2678, doi: 10.1016/j.jmrt.2019.12.095.
- [11] G. Chen, L. Chen, G. Zhao, and B. Lu, Investigation on longitudinal weld seams during porthole die extrusion process of high strength 7075 aluminum alloy, *Int. J. Adv. Manuf. Technol.*, 91 (2017) 5–8, 1897–1907, doi: 10.1007/s00170-0169902-8.
- [12] Z. H. Jia, J. Royset, J. K. Solberg, and Q. Liu, Formation of precipitates and re-crystallization resistance in Al-Sc-Zr alloys, *Trans. Nonferrous Met. Soc. China*, 22 (2012) 8, 1866–1871, doi: 10.1016/S1003-6326(11)61399-X.
- [13] Y. Mahmoodkhani, M. A. Wells, N. Parson, and W. J. Poole, Numerical modelling of the material flow during extrusion of aluminium alloys and transverse weld formation, *J. Mater. Process. Technol.*, 214 (2014) 3, 688–700, doi: 10.1016/j.jmatprotec.2013.09.028.
- [14] A. Dhal, S. K. Panigrahi, and M. S. Shunmugam, Precipitation phenomena, thermal stability and grain growth kinetics in an ultra-fine grained Al 2014 alloy after annealing treatment, *J. Alloys Compd.*, 649 (2015), 229–238, doi: 10.1016/j.jall-com.2015.07.098.

Note: The responsible English translator is the Native Proofreading Service - in Indonesia.